a non-profit environmental and climate research institute

Thormøhlens gate 47, N-5006 Bergen Norway

NERSC Technical Report no. 389

Setting up and testing a regional model for Fram Strait that can be used for the assimilation of acoustic tomography data

by

Florian Geyer, Hanne Sagen, Bruce Cornuelle and Ganesh Kopalakrishnan

Bergen, 15. Juni 2018

Nansen Environmental and Remote Sensing Center
Thormøhlensgate 47
N-5006 Bergen - NORWAY
Phone: +47 55 20 58 00 Fax: +47 55 20 58 01
E-mail: post@nersc.no http://www.nersc.no

a non-profit environmental and climate research center

REPORT

TITLE Setting up and testing a regional model for Fram Strait that can be used for the assimilation of acoustic tomography data.	**REPORT No.** Technical report no. 389
CLIENTS Research Council of Norway ENGIE	**CONTRACTS** Contract no. 226373 Contract no.1000797
CONTACT PERSONS Christine Daae Olseng (NFR) Tom Steinskog (ENGIE)	**AVAILABILITY** OPEN
AUTHORS Florian Geyer, Hanne Sagen, Bruce Cornuelle and Ganesh Kopalakrishnan.	**DATE** 15. June 2018
EXECUTIVE SUMMARY This report presents the regional model Fram Strait model set up for the purpose of assimilation acoustic tomography data from the ACOBAR and UNDER-ICE experiments. The model is evaluated using oceanographic and acoustic observations and is a valuable tool for analyzing Fram Strait oceanography and acoustics.	
APPROVAL *Hanne Sagen, Group leader*	 *Sebastian H. Mernild, Director*

Contents

1 Introduction

In this report, we will describe the results from

1. UNDER-ICE WP 1 concerning using acoustic data to constrain ice-ocean models
2. UNDER-ICE WP 3 estimation of the heat and mass transports through the Fram Strait from a selection of models
3. UNDER-ICE WP 3 estimate the impact of assimilation of acoustic data on the results.

The reported work has been carried out in a collaboration between NERSC, SCRIPPS, and University of Texas-Austin. The external partners contributed hereby as follow: University of Texas-Austin delivered ASTE ocean state estimate fields with a time resolution of 3 days. Scripps set up the high-resolution regional Fram Strait model and helped with running the model and data assimilation.

1.1 Background and Previous work.

Motivation

The environment: The Fram Strait is the only deep-water connection between the world oceans and the area for water-mass and sea-ice transports into and out of the Arctic Ocean (Besczcynska-Möller et al., 2012; de Steur et al., 2009; Langehaug et al., 2013). The flow through Fram Strait is bidirectional and complex, with recirculation of Atlantic Water within the Strait (Marnela et al., 2013) and fronts between the different currents and water masses in the Strait (Walczowski, 2013; von Appen, 2016). It is therefore of peculiar interest for ocean climate monitoring including modelling and observations. Acoustic tomography experiments observed high temporal variability and provided path-depth averaged temperature measurements that are hard to obtain using conventional methods (Dushaw and Sagen, 2016). Data assimilation of these acoustic tomography results is an important goal of the UNDER-ICE project and will likely provide an improved description of water-mass exchanges through Fram Strait

Modelling: Ocean models have traditionally struggled to realistically represent the water mass exchanges through Fram Strait. This causes problems for large-scale models such as climate models to correctly predict the stratification of the Arctic Ocean. The abundance of small-scale variability, such as eddies, in Fram Strait, causes problems for the models to realistically describe the temporal variability in Fram Strait as well as describing processes likely influenced by small-scale variability, such as the recirculation of Atlantic Water in Fram Strait (Hattermann et al., 2016). Recently, high-resolution models have made progress describing the small-scale variability and the water mass circulations in Fram Strait (Wekerle et al., 2017).

Observations: An moored acoustic tomography network in the Fram Strait has been developed in a sequence of three experiments. A single-track experiment in 2008-2009 was carried out as part of the DAMOCLES project 2005-2010 (Skarsoulis et al., 2010; Sagen et al., 2016). This was followed by the implementation of a multipurpose acoustic network (2010-2012) with a triangle of acoustic transceivers for ocean acoustic tomography, ambient noise, and glider navigation (Sagen et al., 2017; Yamakawa et al., 2016). As part of the UNDER-ICE project the thermometry measurements were continued with eight acoustic

paths crisscrossing the Fram Strait from 2014 to 2016. This experiment is documented in detail in Storheim et al. (2018).
In DAMOCLES a new inversion technique was developed by Skarsoulis et al. (2010) based on EOFs. Furthermore, the oceanographic complexity in the Fram Strait has led to refined inversion techniques (Dushaw and Sagen, 2016; Dushaw et al. 2016; Dushaw and Sagen, 2017). This implies that the assimilation approaches need to be modified to adopt to the environmental conditions.

1.2 The ACOBAR experiment

The ACOBAR project (2008-2013) was funded by EU framework programme. An ocean acoustic tomography system consisting of three moorings with low frequency, broadband transceivers forming a triangle was installed in Fram Strait during 2010-2012 (Sagen et al., 2017). The mooring triangle was located in the central, deep-water part of Fram Strait (see Figure 1). The instruments were originally deployed during August-September 2010. During September 2011, A and D were recovered, the batteries replaced, and the moorings redeployed. The final mooring recovery took place during September 2012. The transceivers had Teledyne Webb Research swept-frequency acoustic sources that transmitted linear frequency-modulated (LFM) signals with bandwidths of 100 Hz and center frequencies of approximately 250 Hz. A and C transmitted every 3 hours every other day; B transmitted every 3 hours every day. The data processing is described in Geyer et al., (2015).
Hydrographic data were obtained on a subset of the acoustic paths at various times during the 2010-2012 ACOBAR experiment using either a Sea-Bird 9/11 Conductivity-Temperature-Depth (CTD) or a combination of T-5 (1830 m) and T-7 (760 m) XBT (eXpendable BathyThermograph) probes. These hydrographic measurements provide in situ temperature and salinity that can be used to estimate the sound speed environment between the mooring locations. Objective maps derived from the hydrographic data were used for predicting the acoustic arrivals by forward acoustic modelling.

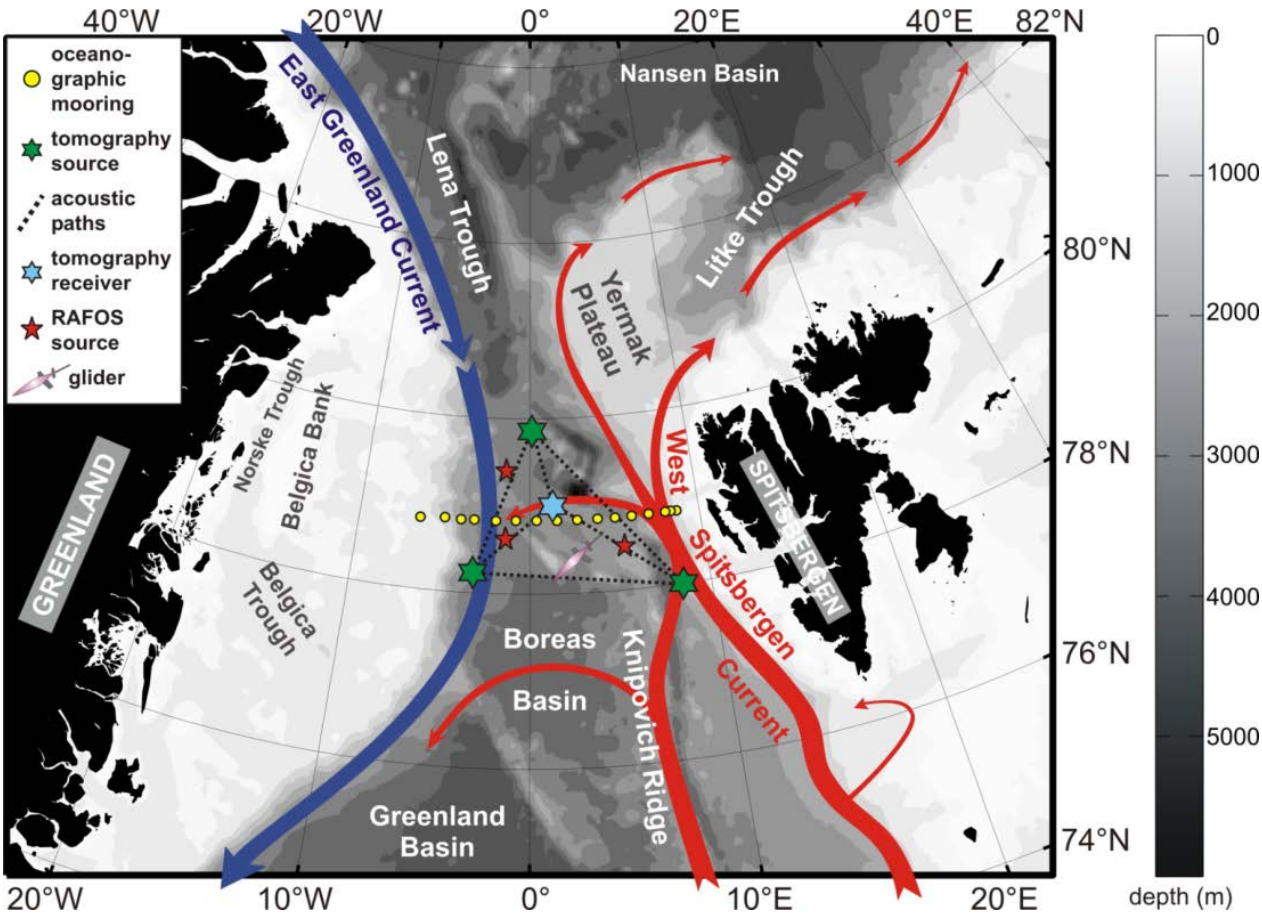

Figure 1: The ACOBAR acoustic thermometry experiment in Fram Strait. The tomographic source moorings (green) are called moorings A, B and C (clockwise from east), the receiver mooring (blue) is mooring D

1.3 Focus of this report: prepare the combination of ice-ocean models with observations

This report focuses on establishing the baseline knowledge needed for modifying the assimilation schemes using the processed and inverted data from ACOBAR, while the UNDER-ICE data will be presented in Storheim, Sagen et al. (2017). The methodologies developed in this project will be used for the UNDER-ICE and the CANAPE project in an upcoming project to be funded by ONR-global.

In this work we will use quality checked acoustic travel times and inverted acoustic data from the from the ACOBAR project, (Sagen et al. 2017, Dushaw and Sagen, 2017).

Chapter 2 of this report will document the need for a new regional model for Fram Strait that realistically describes the vertical stratification in the region and thus correctly represents the ocean sound channel. The setup of this new, eddy-permitting, regional model for Fram Strait is then presented.

Chapter 3 will present the model evaluation against both classic oceanographic data from the AWI/NPI Fram Strait mooring section as well as against timeseries of depth-range averaged temperatures derived by inversion from the ACOBAR acoustic tomography experiment.

Finally, model heat fluxes calculated from the regional model will be compared to the available observational and model data.

Chapter 4 will present acoustic ray modeling based on the regional Fram Strait model and detailed comparisons with observations from the acoustic tomography experiment. These comparisons provide both more evaluation for the regional Fram Strait model as well as new insights into the structure and stability of acoustic arrivals in Fram Strait. This knowledge form the basis for deciding on the observational matrix to use for data assimilation acoustic tomography results in Fram Strait.

2 The regional Fram Strait model

2.1 Available climate models and operational models in Fram Strait: comparison to observations and climatology

2.1.1 Purpose of testing different models for Fram Strait

A main goal of the UNDER-ICE project is the assimilation of acoustic travel times from the acoustic tomography experiments in Fram Strait into an ocean model to improve the estimates of oceanic heat transport into the Arctic. These estimates are highly uncertain at present, with the estimates from measurements having a high statistical uncertainty due to impossibility to cover the high spatial variability in Fram Strait by conventional oceanographic mooring arrays and the model estimates being very widely spread. It is assumed that the integrative nature of acoustic tomographic measurements would greatly improve the estimate of the large-scale mean temperatures and therefore also improve the heat flux estimates.
For an ocean model to be suitable for assimilating acoustic travel times, the model needs to quite accurately represent the vertical sound profiles in the study region. This is important for the model to be able to reproduce the observed acoustic arrival patterns and the underlying acoustic propagation paths. When assimilating acoustic arrivals using a classic ray theory approach, the acoustic ray path is assumed to be constant according to the first-order principles employed in acoustic tomography.

2.1.2 The different models tested in Fram Strait

Several ocean models where tested for the experiment area in central Fram Strait, including the operational TOPAZ model from Met.no and Nansen Center (Sakov et al., 2012), the ASTE state estimate from the ECCO model consortium (Nguyen et al., 2017; building on ECCO v4: Forget, 2015a; Forget, 2015b) and the Norwegian climate model NorESM (Bentsen et al., 2013).
The Arctic subpolar gyre State Estimate (ASTE) is a MITgcm model with 4-DVAR assimilation of ocean and sea ice observations (satellite data). The modelling domain encompasses the Arctic Ocean, the Nordic Sea and the Pacific Ocean north of 47.5°N as well as the Atlantic Ocean north of 32.5°S. It is nested within the ECCO model – version 4, which fits observations well, according to the ECCO consortium. The ASTE state estimate has 50 vertical layers and approximately 14 km horizontal resolution in the Arctic.

2.1.3 Available climatology in Fram Strait

Two main climatological data sets are available for comparison in Fram Strait. Ship-borne measurements are aggregated to gridded climatological data in the World Ocean Atlas. Annual mean data from the newest version of the World Ocean Atlas (WOA13) were used for comparison with the ocean models in Fram Strait as well as for the eventual bias correction of the ASTE state estimates (see chapter 3). A long-term mooring section has been deployed across Fram Strait since 1997, climatology from this long-term monitoring effort was published in Bescszynska-Möller et al., 2013. This data set was used to evaluate large-scale ocean models as well as the bias-corrected high resolution Fram Strait ocean model (see chapter 3).

2.1.4 Results of the comparison

Hydrographic sections taken during along acoustic paths in 2010, 2011 and 2012 as part of the ACOBAR project were used to evaluate the performance of available climatology, operational ocean models and climate models. Special attention was on the vertical sound speed profiles, because a correct description of the ocean sound channel is essential to successfully model the acoustic paths of the ACOBAR acoustic tomography experiment. World Ocean Atlas climatology and the snapshots of the hydrographic measurements agreed on the main features of the vertical sound speed profiles such as cold surface channel (sound speed minimum) in western Fram Strait, a warm Atlantic layer connected to the West Spitsbergen Current in eastern Fram Strait (sound speed maximum), a warm recirculation layer in western Fram Strait and the main sound channel (sound speed minimum) below the Atlantic layer (Figure 2, Figure 3). Deviations between climatology and the hydrographic sections were largest in western Fram Strait, where observations are scarce, and in the surface layer, where temporal variability is largest.

The ocean models, however, showed large deviations from both hydrographic measurements and climatology. The main deviation in addition to depth-independent offsets (most prevalent in the NorESM climate model) were very large depth-dependent offsets (most prevalent in the TOPAZ operational ocean model and the ASTE ocean state estimate), such as cold surface layers in eastern Fram Strait (ASTE, Figure 2 and Figure 3 right panel), a too high temperature maximum at an incorrect depth for the Atlantic layer (TOPAZ and ASTE, Figure 2, Figure 3 right panel), too far westward extension of warm Atlantic water in Fram Strait (TOPAZ and ASTE, Figure 8 left panel), and an incorrect sound channel depth (TOPAZ, Figure 7).

The deviations of all tested models were altogether too large to allow realistic acoustic modelling on the model fields provided for the ocean models. It was therefore concluded that any model fields would need to be bias-corrected against climatology before being used as boundary condition to a high-resolution regional Fram Strait model. Despite its large deviations the ASTE ocean state estimate was chosen to provide the boundary conditions, because it had a correct sound channel depth and sound speed minimum and because it was the easiest model to technically implement, being a z-level model based on the same code (MITgcm) as the high-resolution regional Fram Strait model.

The bias correction of the boundary conditions will make the high-resolution regional Fram Strait model aligned with climatology, while still getting the variability described by the ASTE state estimate in the boundary conditions. Because the bias-correction only applies to the boundary conditions, the regional Fram Strait model will still be internally consistent.

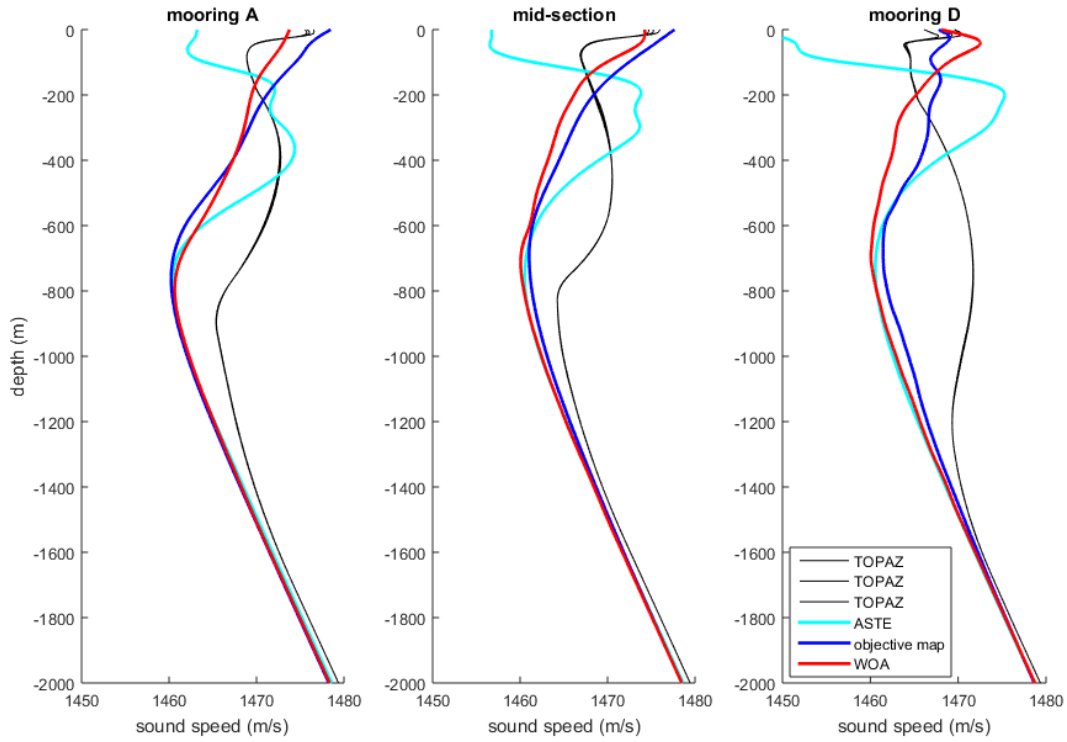

Figure 2: Comparison of temperature stratification for ACOBAR section A-D in eastern Fram Strait. Objective map from hydrographic instruments (blue), World Ocean Atlas 13 climatology (red), TOPAZ operational ocean model (black), ASTE ocean state estimate (cyan).

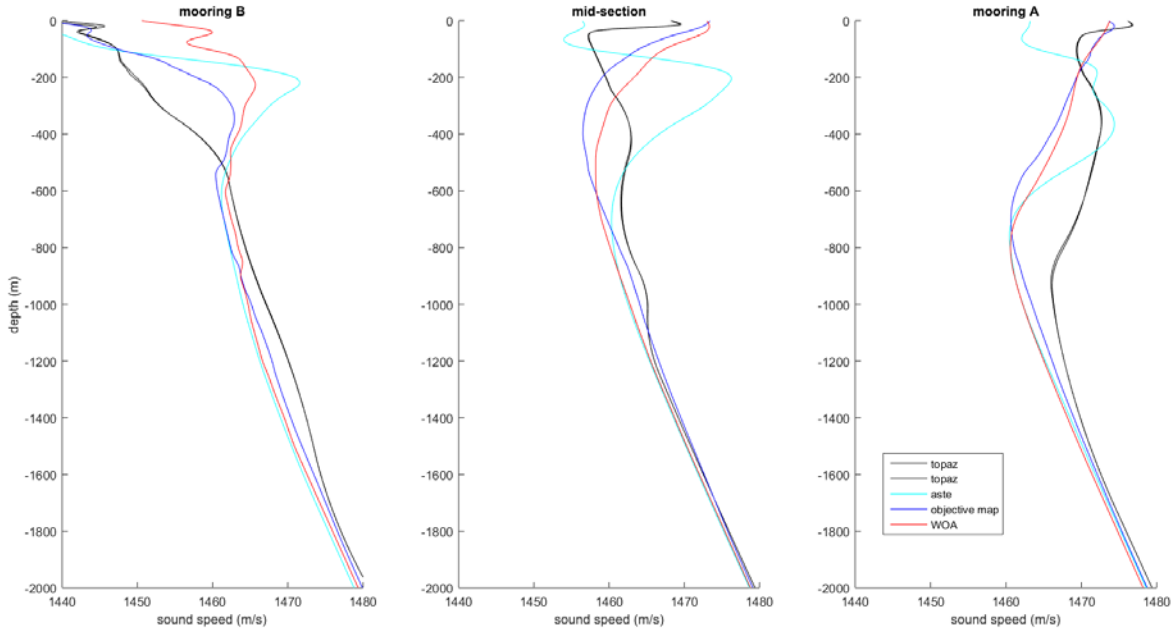

Figure 3: Comparison of temperature stratification for ACOBAR section B-A, which crosses Fram Strait from west (station B) to east (station A). Objective map from hydrographic instruments (blue), World Ocean Atlas 13 climatology (red), TOPAZ operational ocean model (black), ASTE ocean state estimate (cyan).

2.2 A new high-resolution z-coordinate model for Fram Strait and its use for acoustics

2.2.1 The MIT model setup for Fram Strait

A regional z-coordinate model was set up for Fram Strait. The model employed is the MIT general circulation model, using a horizontal Arakawa C-grid and 52 depth layers. The model domain covers the area from 72°93'N to 82°07'N and from 19°30'W to 19°30'E. The depth layers are most densely spaced close to surface with 12 layers within the first 100 m depth and 20 layers within the first 200 m depth. The horizontal resolution is 4.6 km in North-South direction. In East-West direction it varies from 3 km at the northern boundary to 6.5 km at the southern boundary.

The ASTE state (Nguyen et al., 2017) estimate provided initial and boundary conditions for the regional z-coordinate model. It is itself nested in the global ECCO model (The ECCO Consortium, 2017a; The ECCO Consortium, 2017b). As discussed in chapter 3 the vertical stratification of the ASTE state estimate, just as that of all other models tested, was not sufficiently accurate in Fram Strait to allow realistic acoustic modelling. Therefor the ECCO model data was bias-corrected with respect to climatology. This was done by comparing the long-term mean (2010-2012) field of the ASTE data with the annual mean climatology as provided by the World Ocean Atlas 2013 (WOA13). To do this both the ASTE state estimate and the WOA13 climatology fields were interpolated onto the regional Fram Strait model grid. The temperature and salinity difference between the two mean fields was subtracted from the interpolated ECCO model data at all time steps to correct for the bias. There bias-corrected interpolated ECCO fields were then used as initial and boundary conditions for the regional Fram Strait model, using a 10-grid point wide sponge layer for the boundary conditions. For better control, only the northern, southern and eastern boundaries were treated as open boundaries. The fluxes at the boundaries were corrected to be identical than the ECCO model fluxes at the respective boundaries to correct for interpolation errors.

A snapshot of the model results (Figure 4) shows the main circulation features in Fram Strait. The warm West Spitsbergen Current flows northward along the western edge of the Svalbard shelves. It splits on the northwestern corner of Svalbard into two branches. One branch continues northwards along the western edge of the Yermak plateau, the other branch crosses the Yermak plateau eastwards and flows eastwards along the northern shelf edge of Svalbard. Throughout Fram Strait the West Spitsbergen current sheds eddies on its western side feeding a recirculation of warm Atlantic Water within Fram Strait. The eddy shedding and recirculation is most intense between 78 and 81°N. On the western side of Fram Strait cold polar waters flow south in the East Greenland Current. This current is strongest of the eastern Greenland shelf edge.

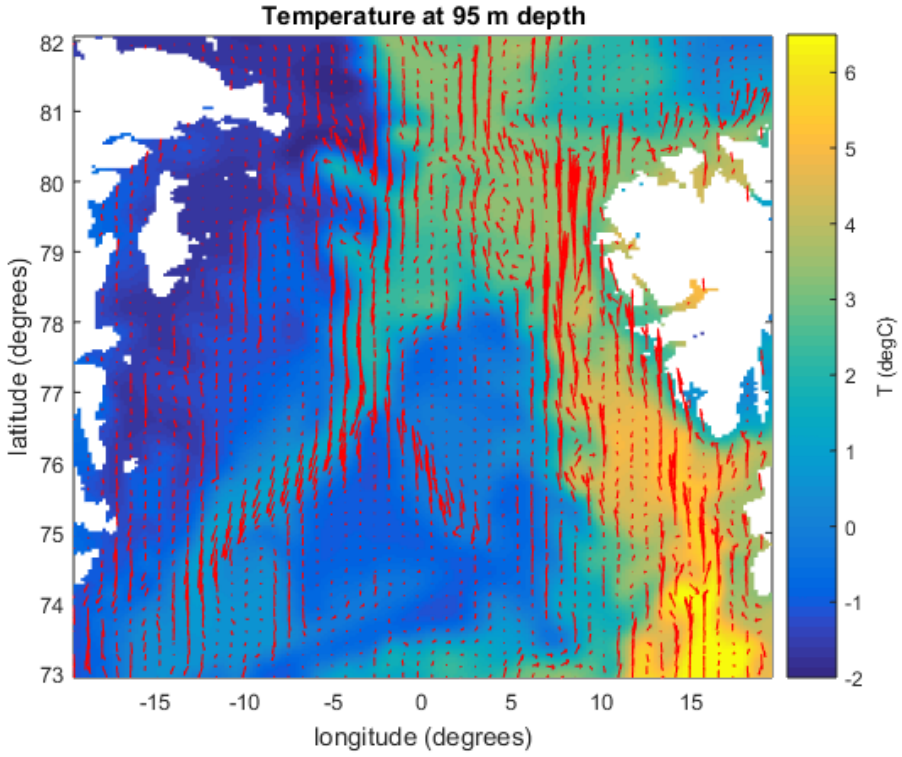

Figure 4: Snapshot of Fram Strait model results. Temperatures and currents at 95 m depth on 12. September 2010, concurrent with hydrography measurements of ACOBAR section A-B. For better clarity only every fifth velocity vector in each direction is plotted.

3 Model evaluation

3.1 Comparison with Fram Strait mooring section

The model results from the regional Fram Strait model were compared to the Fram Strait climatology as measured by the 78°50'N mooring section across Fram Strait (Bescszynska-Möller et al., 2013) maintained by the Alfred Wegener Institute, Bremerhaven (AWI) and the Norwegian Polar Institute in Tromsø (NPI). The distribution of warm Atlantic Water and Atlantic Recirculated Water is greatly improved in the Fram Strait model compared to the ASTE state estimate (Figure 5). In ASTE the warm water in the West Spitsbergen current extended too deep (a common problem in both operational ocean models and climate models), as well as extended much too far west in Fram Strait. In the Fram Strait model the lower boundary is realistic, the extent of warm water is corrected, if seemingly slightly overcompensated. The Fram Strait model also shows a slight temperature maximum at 300 m depth in western Fram Strait that is present in the climatology. However, the cold surface water in western Fram Strait is not cold enough in the Fram Strait model. This area is insufficiently sampled in measurements, especially during winter. Thus, the World Ocean Atlas likely was biased in this region. The slightly too cold Atlantic layer temperatures in central Fram Strait are consistent with the modeling efforts by Wekerle et al. (2017) that demonstrated that even higher horizontal resolutions were necessary to reproduce the full strength of eddy shedding from the West Spitsbergen Current into the central recirculation region.

The current field across the Fram Strait mooring section was also improved in the Fram Strait model relative to the ASTE state estimate (Figure 6). This is especially the case for the northward West Spitsbergen current in eastern Fram Strait. In the ASTE state estimates the current was too weak and too far onshore. Again, there might be slight overcompensation in the Fram Strait model. The highly variable current field in the recirculation region of central Fram Strait shows a similar banded structure in the Fram Strait model as observed in the mooring measurements, the differences can be attributed to the simplified bottom topography caused by the limited model resolution. The ASTE model had shown no banded velocity structure in central Fram Strait. It should be noted here that the initial and boundary currents in the Fram Strait model are not bias-corrected as no three-dimensional climatology of ocean currents exists. Therefore, the current field improvements are solely due to improvements in the density fields and in the slightly finer bottom topography employed in this model. While the southward East Greenland Current in western Fram Strait was too shallow in the ASTE state estimate, it tends to be rather too barotropic in the Fram Strait model. The maximum velocities of the East Greenland Current close to the ocean surface were improved in the Fram Strait model compared to the ASTE state estimate.

In general, the setup with bias-corrected initial and boundary condition from the ASTE state estimate driving the high-resolution regional Fram Strait model turned out to be successful. It reproduces both the general mean circulation in Fram Strait and the vertical stratification and thus the vertical sound speed profiles in Fram Strait. As shown in chapter 2.1 none of the available operational ocean models, state estimates or climate models had achieved that. It is a necessary condition for the successful assimilation of acoustic tomography data into an ocean model. We chose not to assimilate travel-times directly, however, due to the complication of the acoustic paths, and instead used an approximate pre-inversion for range-averaged sound-speed and assimilated these averages (see chapter 4).

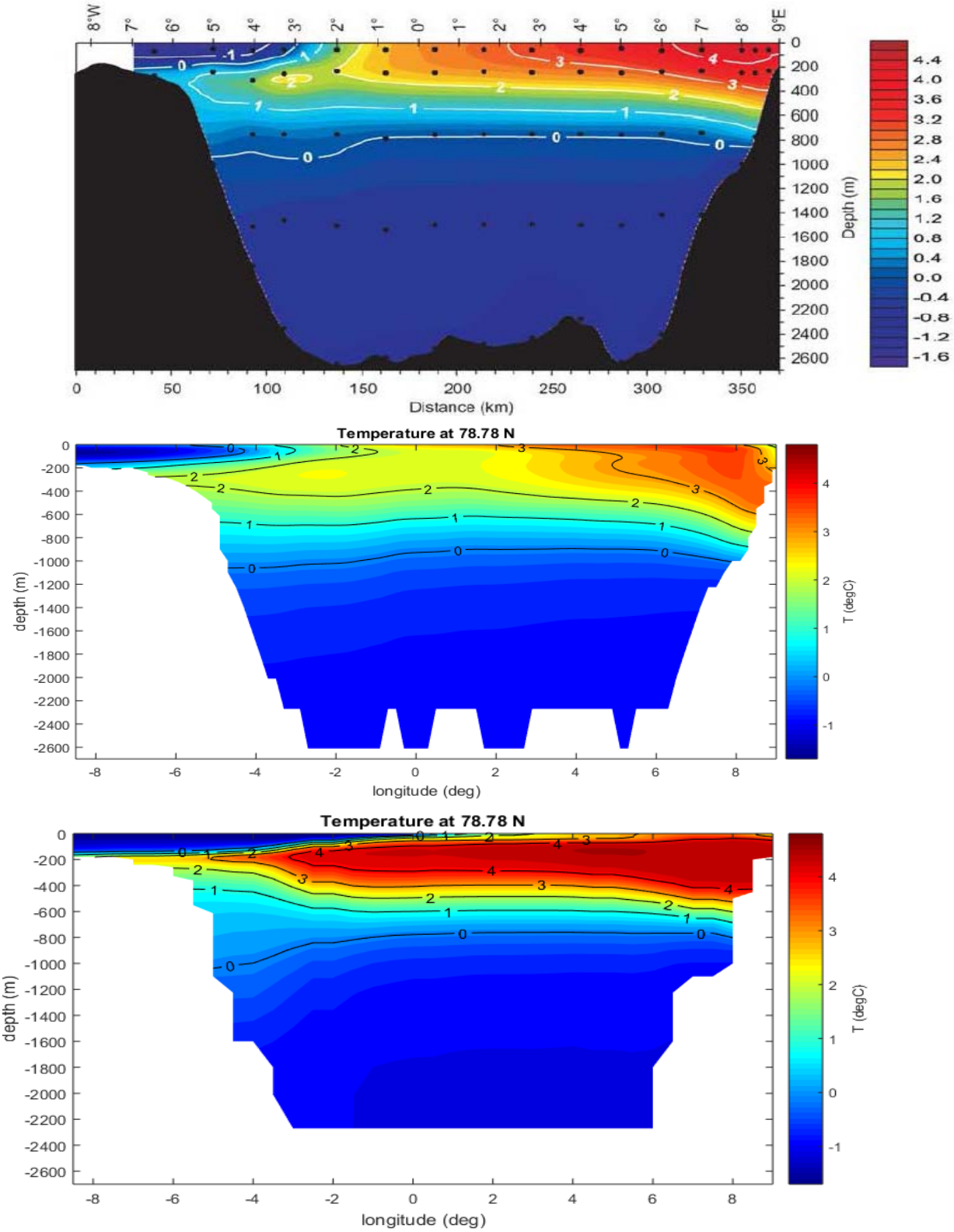

Figure 5: Fram Strait temperature cross-section at 78°50'N. Upper panel: long-term mean interpolated mooring measurements (2002-2008). Middle panel: mean model results from Fram Strait MIT model (2010-2012). Lower panel: mean model results from ASTE state estimate (2010-2012).

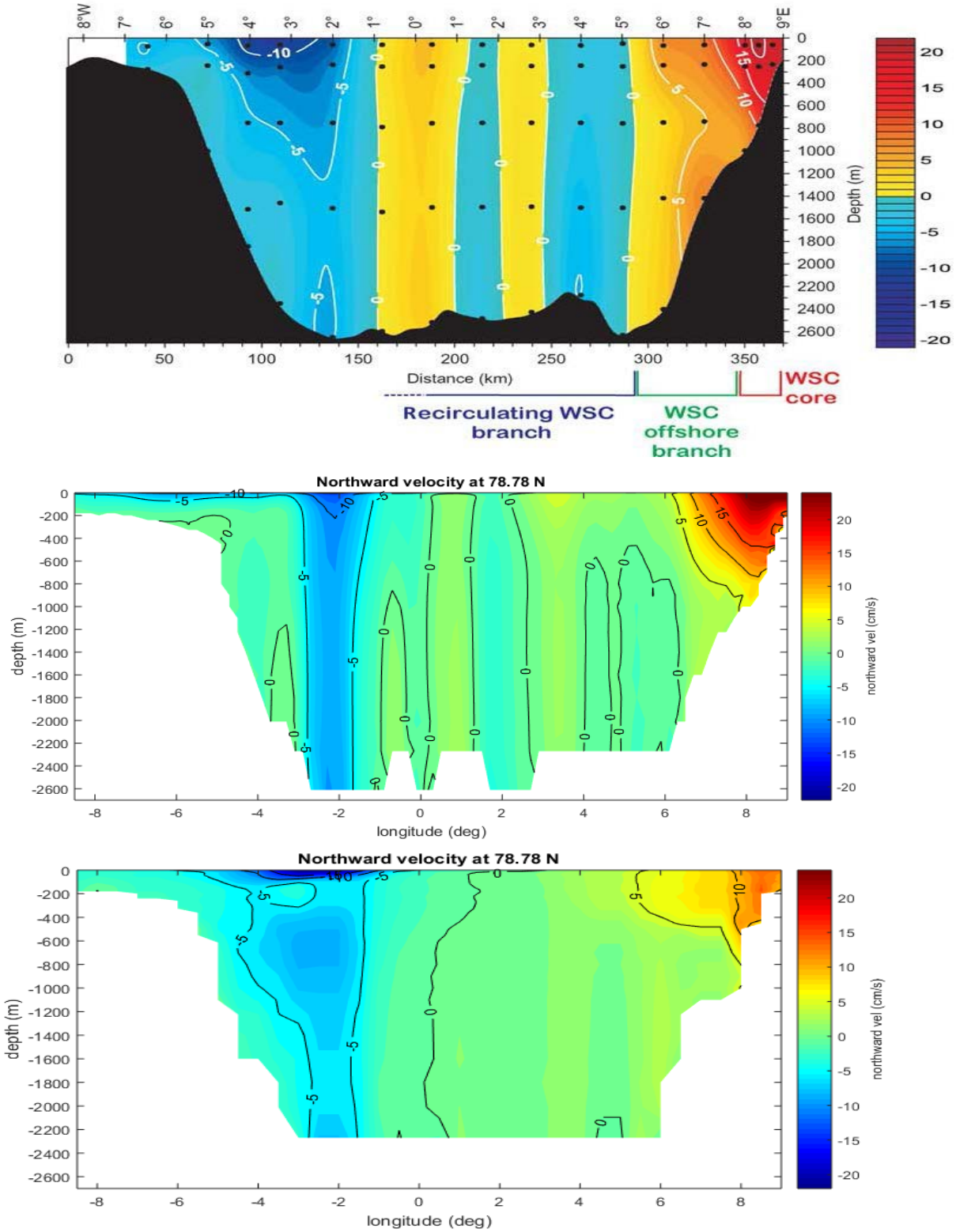

Figure 6: Fram Strait northward velocity cross-section at 78°50'N. Upper panel: long-term mean interpolated mooring measurements (2002-2008). Middle panel: mean model results from Fram Strait MIT model (2010-2012). Lower panel: mean model results from ASTE state estimate (2010-2012).

3.2 Comparison of model temperatures with inversion results from acoustic tomography

Chapter 3.1 dealt exclusively with the mean circulation of Fram Strait. In this chapter the Fram Strait model is evaluated against time series of temperature derived from the ACOBAR acoustic tomography experiment. These time series were obtained by Dushaw (2017) using inversion techniques on acoustic travel times along three paths between acoustic source and receiver moorings. The temperatures obtained by the inversion are range averaged along the acoustic paths and depth averaged over a depth range of 0-1000 m.

The modelled temperature fields from the high resolution Fram Strait MITgcm model were interpolated onto the acoustic paths of the ACOBAR experiment and the 0-1000 m depth and range-averaged temperatures were compared to the inversion results from the ocean acoustic tomography experiment (Figure 7). The results from the regional Fram Strait model were clearly an improvement from the ASTE state estimates. For both section B-A and B-D the model results were closer to the inversion results from acoustic tomography than the World Ocean Atlas data, which had been used as a baseline in the inversion calculations and which had been used for the bias correction of the model boundary conditions. The regional model results show signs of an annual cycle similar to those observed in the measurements. There seems to be some temperature drift in the model results. Most likely this drift stems from the ASTE state estimate which exhibits a similar drift. The regional model shows more short-term variability as the lower-resolution ASTE state estimate. The regional model results still strongly underestimate the short-term variability observed in the temperature inversions from acoustic thermometry. According to Wekerle et al. (2017), even higher horizontal resolution than employed by our regional model would be necessary to get a realistic description of eddy-induced short-term variability in Fram Strait.

The quality of the regional model results justifies hopes that 4 DVAR assimilation of range-depth averaged temperatures or sound speeds can be meaningful and successful. It will be interesting to see if the assimilation will only improve the remaining biases of the regional Fram Strait model or also increase the short-term temperature variability.

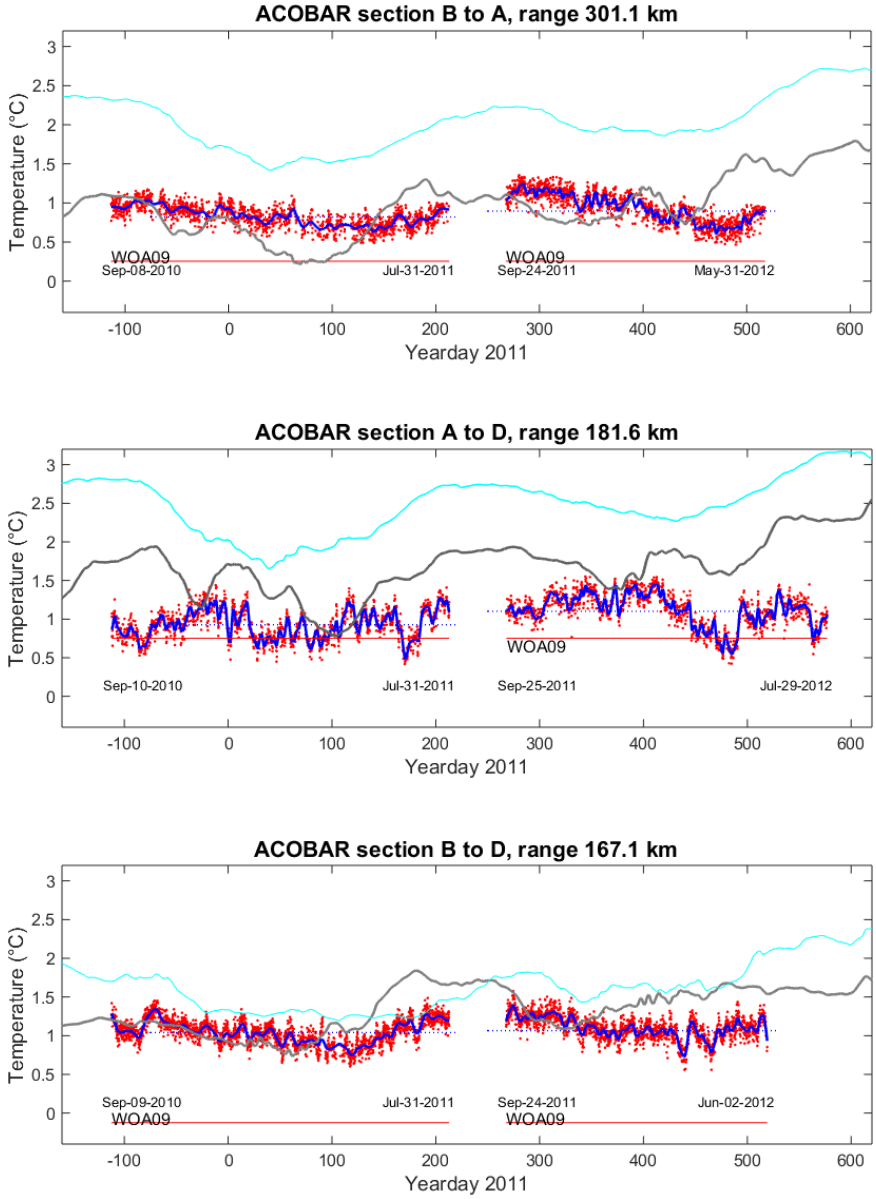

Figure 7: Comparison of range-depth integrated temperatures (0-1000 m depth) along the three acoustic sections of the ACOBAR acoustic thermometry experiment. Inversion results from acoustic tomography (red: raw data, blue: cubic-spline smoothed time series), Fram Strait MIT model results (gray), ASTE state estimate (cyan), World Ocean Atlas climatology (red).

3.3 Heat fluxes

3.3.1 Calculation of heat fluxes in the Arctic

Heat fluxes into an ocean basin always need to be calculated relative to set temperature T_0 as long as no complete budget of all the fluxes in and out of the basin is available. In the case of a closed budget, the appropriate choice would be the average temperature of the ocean basin. In the absence of a closed budget and an accurately determined average Arctic Ocean temperature, the T_0 needs to be chosen arbitrarily (while T_0 = 0 K would be the physically correct, it is not commonly used in geophysics). For the Arctic as value of T_0 = 0 °C is commonly used. With temperatures T and cross-section velocities v known in an ocean model, the model heat flux can be calculated as

$$F = \iint (T(x,z) - T_0)\, v(x,z)\, \rho(S,T,z)\, c(S,T,z)\, dxdz$$

where ρ is the density of seawater and c the specific heat capacity of seawater. The Fram Strait heat flux was calculated at a Fram Strait cross section at 78°49'N and 9°30'W to 9°30'E corresponding to the AWI / NPI Fram Strait oceanographic mooring section.

3.3.2 Comparison of heat fluxes from different models and measurements

Figure 8 shows the poleward heat flux through Fram Strait. The heat flux in the regional Fram Strait model is increased compared to the ASTE state estimate. The variability of the two models is however very similar. Table 1 compares the model heat fluxes to heat fluxes calculated from both mooring measurements and climate models (Ilicak et al. 2016). Both the ASTE state estimate and the regional Fram Strait model have larger northward heat fluxes than the literature values. The variability of our modelled heat fluxes is also much larger than those reported from climate models. This however is to be expected, because of the low spatial resolution of the climate models.

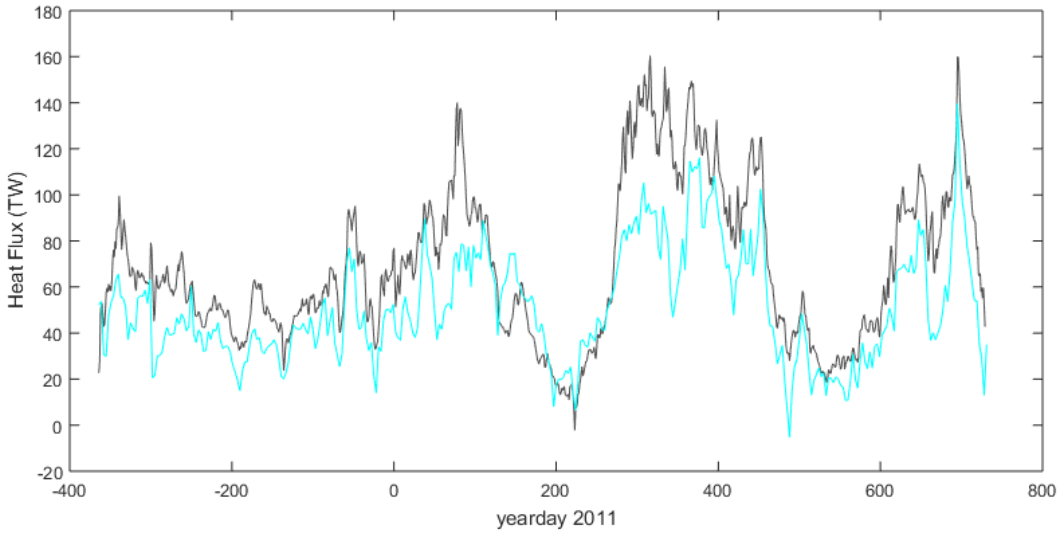

Figure 8: Heat flux across Fram Strait at 78°50'N. Results for regional Fram Strait model (dark gray) compared to ASTE state estimate (cyan). Time resolution for the two models is daily (Fram Strait MIT model) and every three days (ASTE).

Model	Mean heat transport [TW]	Standard Deviation [TW]
Observed	26-50	
ASTE	50.98	24.09 (daily)
Fram Strait MIT model	69.12	33.35 (daily)
Multi Model Mean (Ilicak et al. 2016)	22.98	8.35 (interannual)

Table 1: Comparison of heat fluxes across Fram Strait from observations and models

4 Acoustics in Fram Strait: measurements and modeling

4.1. Structure and stability of arrivals in Fram Strait

4.1.1 Arrival Structure for section A-D

The ACOBAR acoustic tomography section A-D, covering eastern Fram Strait, displayed the most well-defined acoustic arrival pattern, with 20 identifiable arrivals. Several of these arrivals were trackable and presented in Sagen et al. (2017). Because the amount of discernible detail in the arrival structure of this section, it provides a good test case for the performance of acoustic models both based on hydrographic measurement as well as based on numerical ocean models. In addition, it provides a good data series for studying the time variability of acoustic arrivals and the stability or instability of the corresponding ray paths. The arrival structure of this section was used for comparisons to the regional Fram Strait model in the following chapters and is therefore described here in detail.
Based on hydrographic measurements in September 2011 and July 2012 the acoustic arrivals for ACOBAR section A-D were predicted using two different acoustic models. Broadband, range-dependent parabolic equation (PE) modelling (Collins, 1993) gives the most realistic prediction of the acoustic arrivals including an approximation of the relative strength of arrivals. Geometric ray modelling misses shadow arrivals and might also miss very weak arrivals due to their small window in emission angles. Ray modelling will however give the estimated acoustic paths connected to each acoustic arrival, thus allowing to study the stability of the path characteristics.
The forecasted arrival structure from the PE model forecast very accurately corresponds to the measured acoustic arrivals (Figure 9). Main differences are a shift of approximately 70 ms between forecast and arrival and the wider shape of the measured arrivals. The delay can be ascribed to the unknown source delay and errors in the interpolated hydrographic sections. The wider spreading of measured arrivals in time as opposed to the very narrow modelled arrivals is due to acoustic scattering by small-scale ocean variability, which is not captured in the smooth interpolation of the hydrographic section, as it is not feasible to sample hydrographic section densely enough to resolve the small-scale variability in Fram Strait. The effect of this scattering was studied by Dushaw and Sagen (2017). A comparison of the acoustic arrivals predicted by geometric rays to the PE predictions and measurements shows that the ray model captures the arrival structure well, but that most arrivals do not correspond to single rays, but rather to families of rays. Ray modelling also shows that only the first two predicted arrivals correspond to purely refracted acoustic rays. All the later arrivals are bottom-reflected and often surface reflected (SRBR). The arrivals and the basic characteristics of their corresponding ray families are listed in table 2. The spreading of arrivals into ray

families points to the complications of rays in a complex oceanographic environment. Maybe these arrivals could be better described using travel-time sensitivity kernels (Skarsoulis and Cornuelle, 2004) or statistical models accounting for the effect of scattering from small-scale ocean variability (Dushaw and Sagen, 2017).

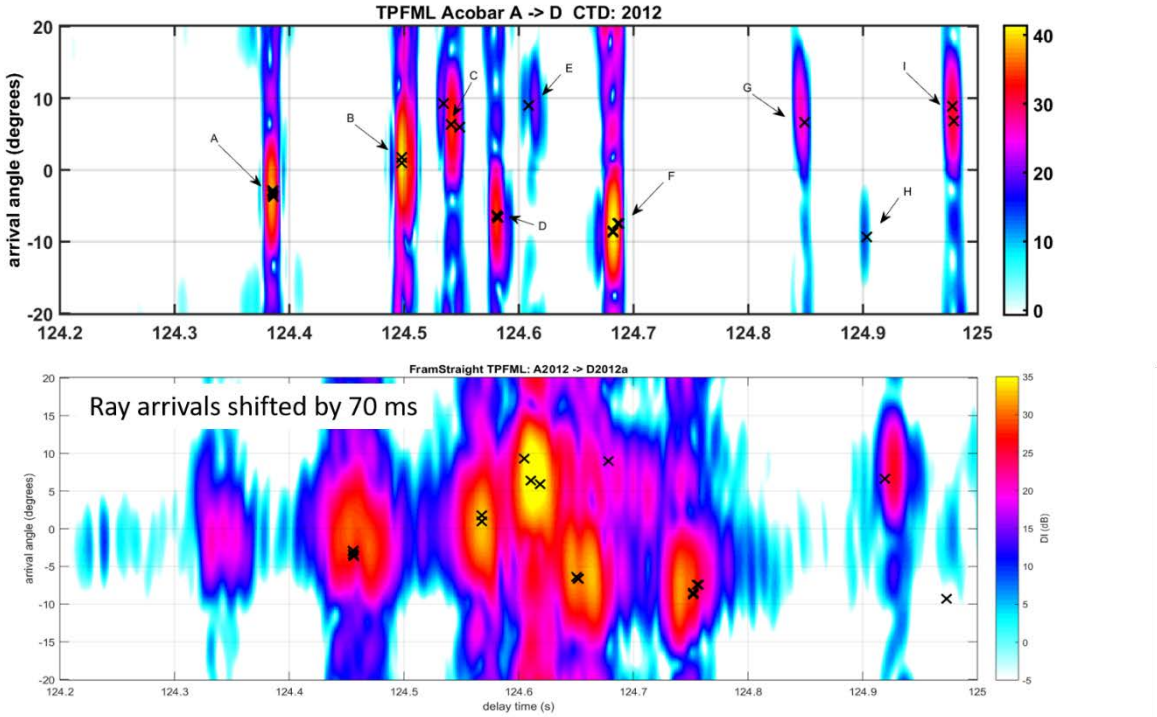

Figure 9: Comparison of predicted arrival (upper panel) and measured arrivals (lower panel) at ACOBAR section A-D. In the upper panel the color code denotes results from a parabolic equation model, crosses denote geometric ray results. In the lower panel denote the measured intensity after matched filtering and estimator-correlator. Crosses denote the ray model results shifted by 70 ms.

Arrival (names by ascending travel time)	Number of bottom reflections / lower turning points	Number of surface reflections / upper turning points
A	4	5
B	5	4
C	5	4
D	5	5
E	5	5
F	5	6
G	6	5
H	6	6
I	6	6
J	6	7
K	6	6
L	6	7
M	7	6
N	Not present in ray model	Not present in ray model
O	7	6
P	7	7
Q	7	7
R	7	8
S	7	7
T	7	8

Table 2: Identifiable arrivals for ACOBAR acoustic section A-D and their general characteristics

So how stable are these families of rays? Comparison of predicted time fronts from September 2011 and July 2012 shows that the time fronts of all bottom reflected arrivals are very stable (Figure 10, Figure 11). The early, purely refracted, arrivals however show extensive variations between the two years, causing the relative timing of the first two arrivals to be variable. For the later arrivals the main variability consists of amplitude variation causing some of the (anyway low-power) arrivals to be missed occasionally (Figure 12). As shown in Sagen et al. (2017), they can be consistently tracked for the whole deployment period despite occasional drop-outs because their overall pattern is so stable.
Looking at details of the predicted ray paths however points to instabilities of bottom-refection positions and of instabilities of narrow bottom misses, i.e. near-grazing bottom refraction vs. bottom reflection (Figure 13). These seem not to influence travel times too much, so that the basic ray family characteristics are determining the stable arrival patterns despite these ray path instabilities. Again, these results point to the possible necessities of more complex models than simple ray models to correctly describe sound transmission in Fram Strait. Statistical models or sensitivity kernels possible ways to implement data assimilation of acoustic travel times. A different approach is to assimilate depth-range averaged temperatures or sound speeds obtained by inversion of acoustic travel times instead, thus separating the problem of stable ray paths from the data assimilation.

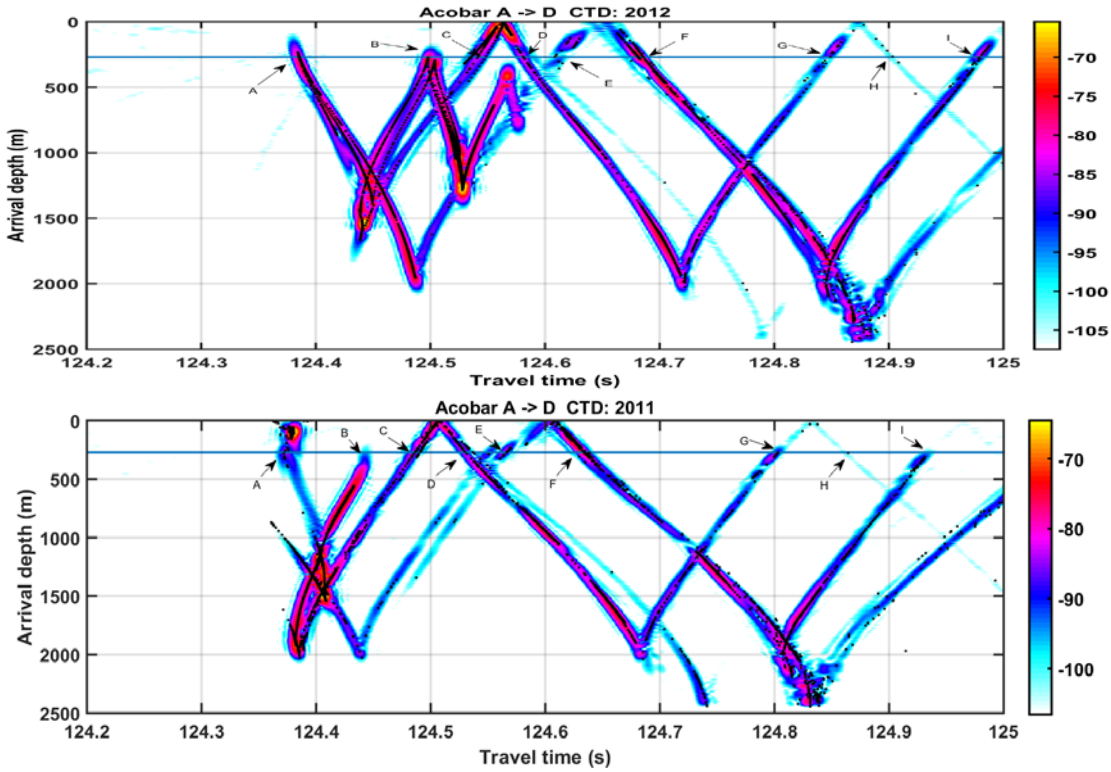

Figure 10: Comparison of early arrivals 2011 vs. 2012 at ACOBAR section A-D

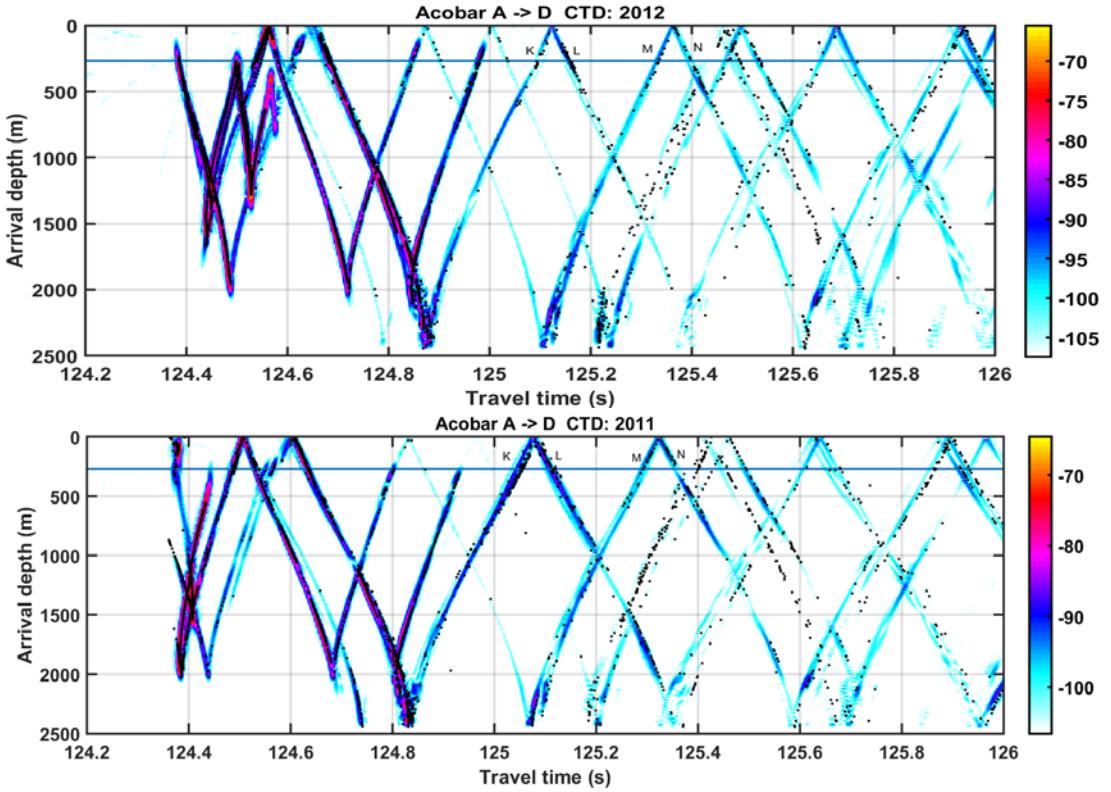

Figure 11: Comparison of late arrivals 2011-2012, modelled timefronts for ACOBAR section A-D

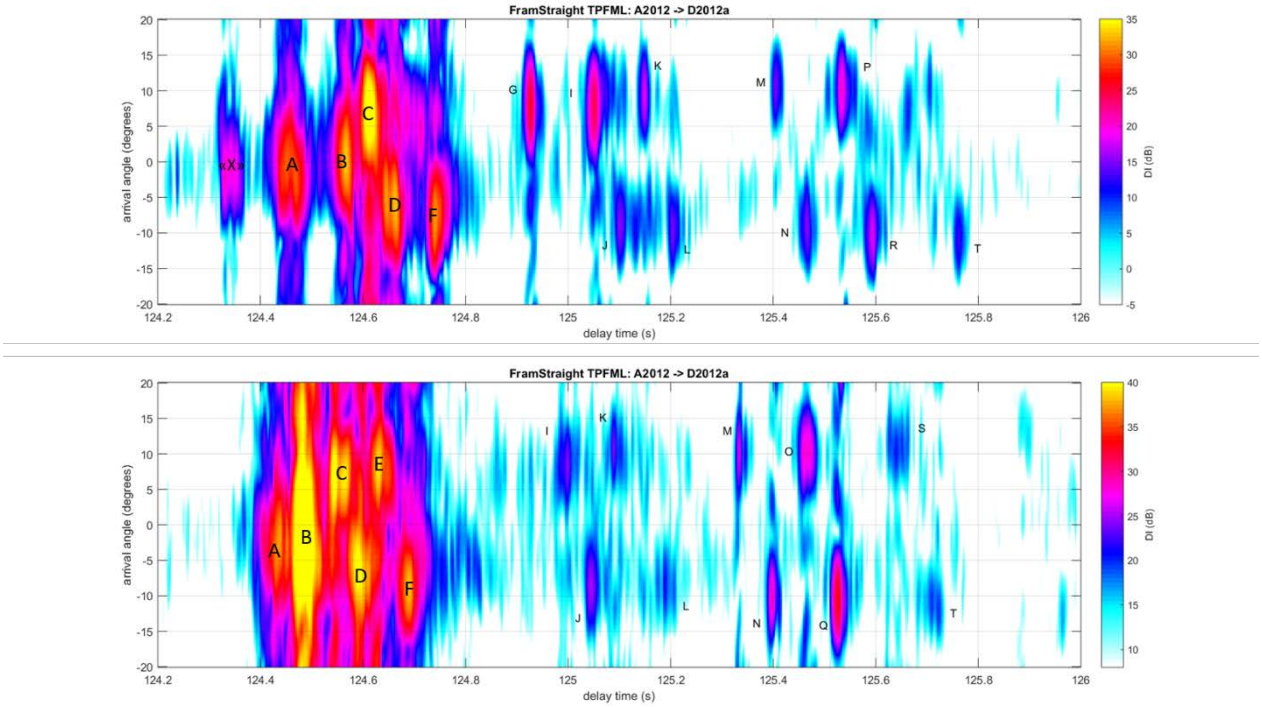

Figure 12: comparison of observed arrivals 2011-2012.

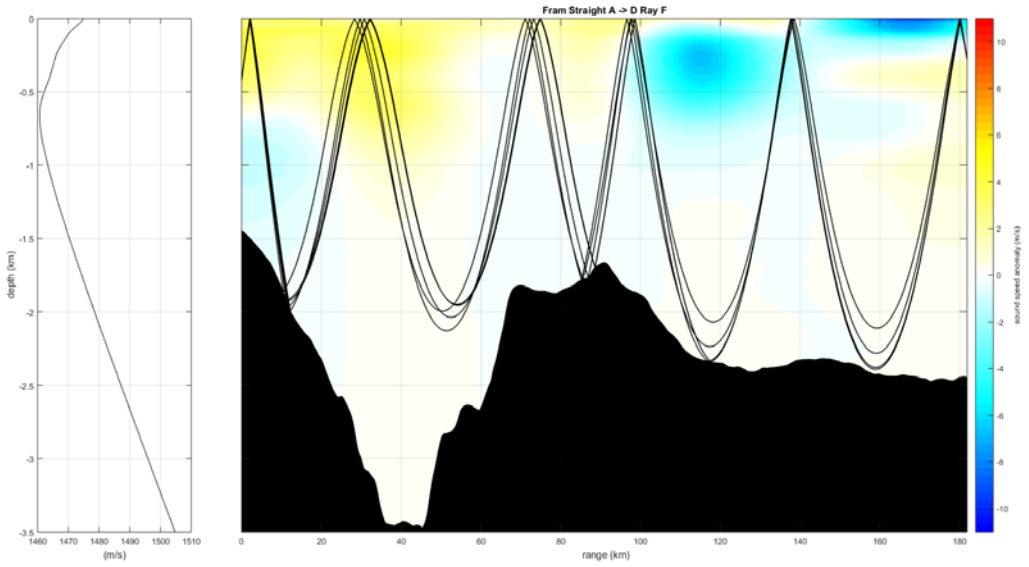

Figure 13: Predicted ray path for arrival F of ACOBAR section A-D, based on CTD section from September 2011. The ray path is ambiguous with respect to the 4th bottom reflection / lower turning point.

4.2 Acoustic results of Fram Strait model

4.2.1 Ray modelling based on the Fram Strait model

Acoustic forward modelling on the high-resolution Fram Strait model was carried out using geometric rays. A comparison of the predicted acoustic timefronts from forward model runs on both Fram Strait model and observed hydrography proved that it was possible to reproduce the observed acoustic arrival patterns (Figure 14), the most important prerequisite to data assimilation.

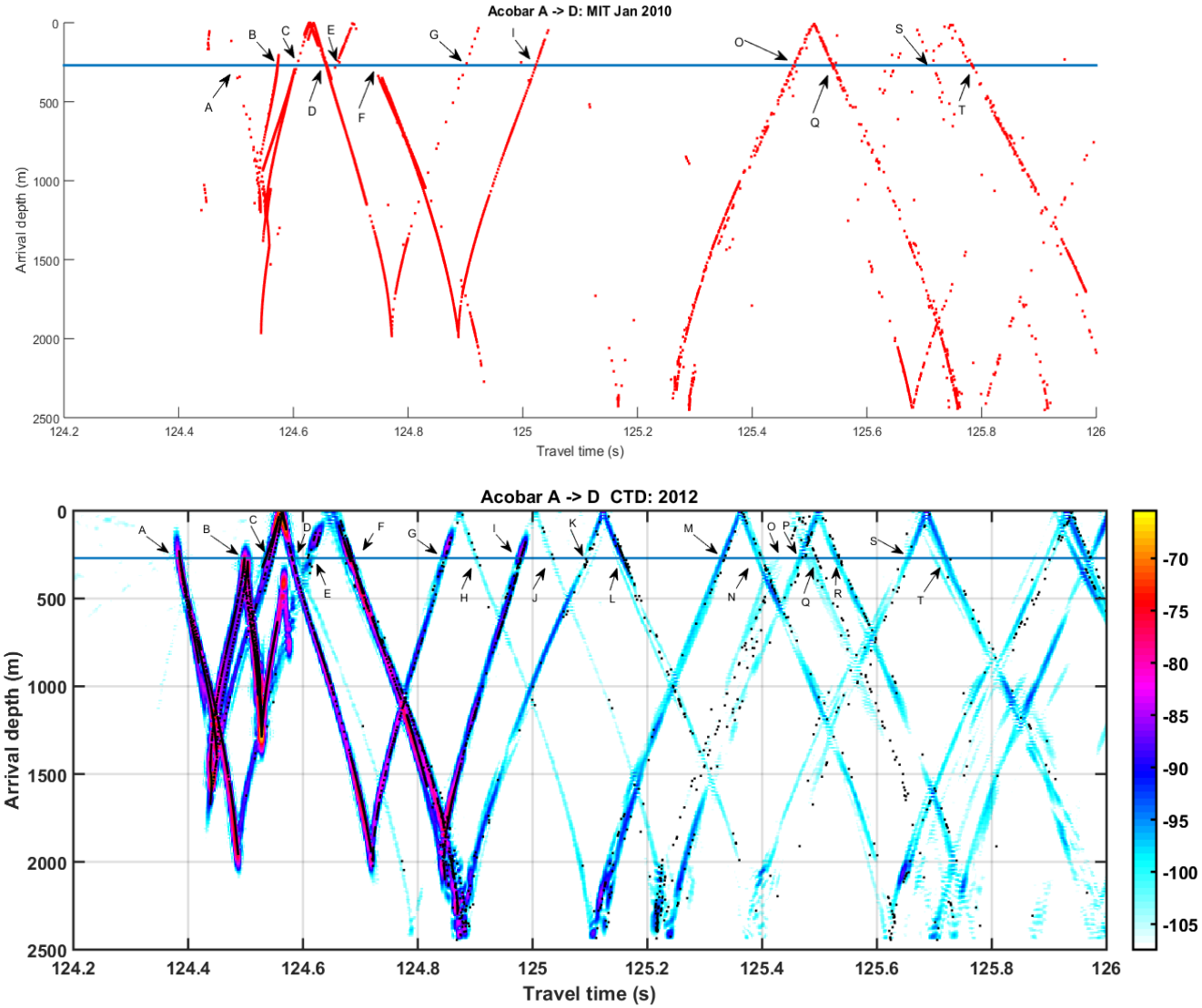

Figure 14: Timefronts predicted from regional Fram Strait model (January 2010, upper panel) compared to time fronts predicted from CTD section (July 2012, lower panel).

The acoustic forward modelling also managed to reproduce the predicted acoustic propagation paths within the range of their natural variability (Figures 15-20). This means that the ocean model is now of sufficient quality for use in data assimilation. This range of natural variability for the ray paths, however, is substantial as none of the predicted rays is strictly speaking stable due to the very strong mesoscale variability in Fram Strait. This means that more realistic descriptions of arrivals than single ray paths are needed as a kernel for

assimilation of acoustic tomography data in Fram Strait. Possible approaches for ray-based assimilation include a statistical approach employing multiple ray paths developed by Dushaw and Sagen (2017) or an approach using travel-time sensitivity kernels (Dzieciuch et al., 2013). Alternatively, inversion results by Dushaw and Sagen (2017) and Dushaw (2017) based on the measured tomographic timeseries (Sagen et al., 2017) can be used to assimilate range-depth averaged temperatures instead of acoustic travel times. Model-observation comparisons of acoustic travel times can then be employed to assess the effects of the data assimilation.

In addition to the comparison to hydrography, forward model results based on the regional Fram Strait model were also compared with the acoustic observations from the ACOBAR experiment (Sagen et al., 2017). Despite a light model drift the comparison revealed striking similarities in the structure and seasonal variability of model and observations, with the overall arrival structures displaying a high degree of stability. There were hints of a seasonal cycle at sections AD and BA. Both model and observation show cooling events where the early sound channel arrivals overlap or cross the later bottom-reflected arrivals. Both model and observations show addition early sound channel arrivals during warming events.

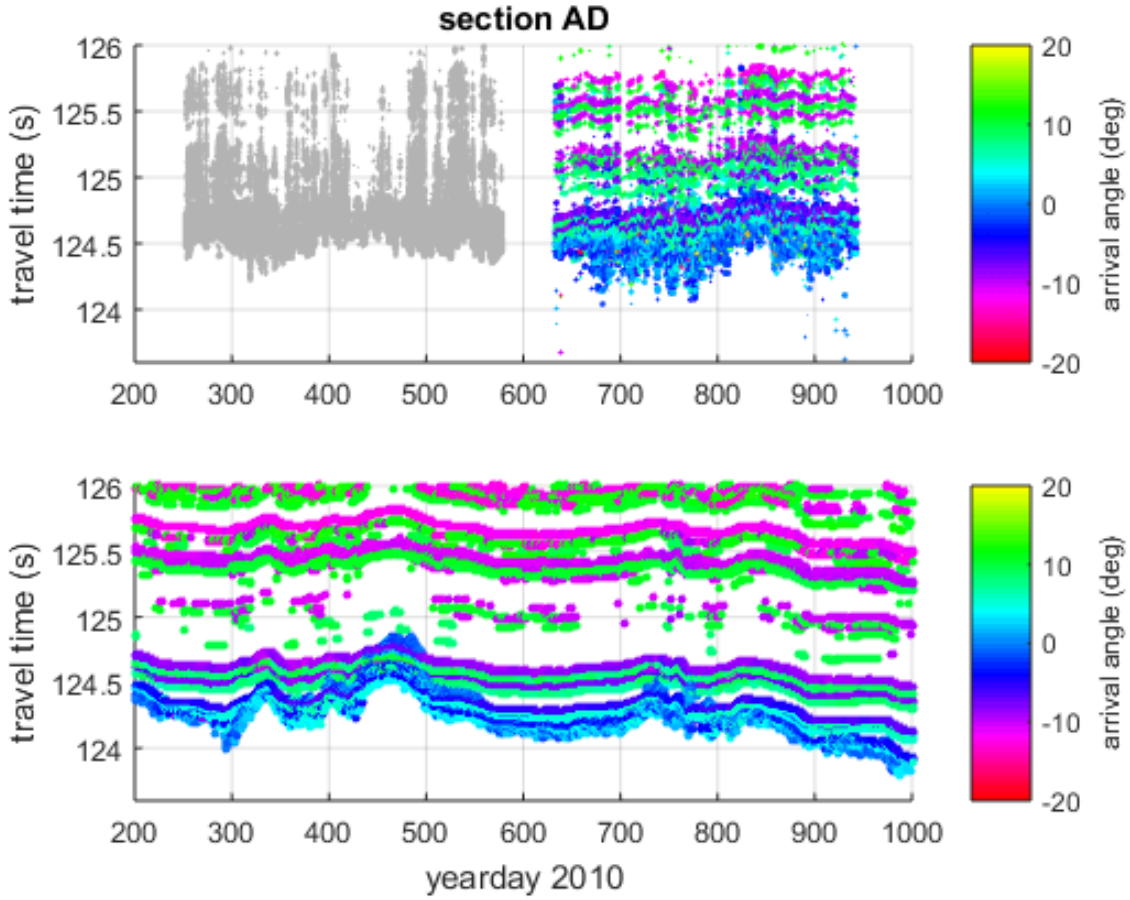

Figure 15: Observed time series of acoustic arrivals for ACOBAR section AD (upper panel) and predicted time series of arrivals for section AD from regional Fram Strait (lower panel). For the first deployment year of section AD no arrival angle information is available for the observations.

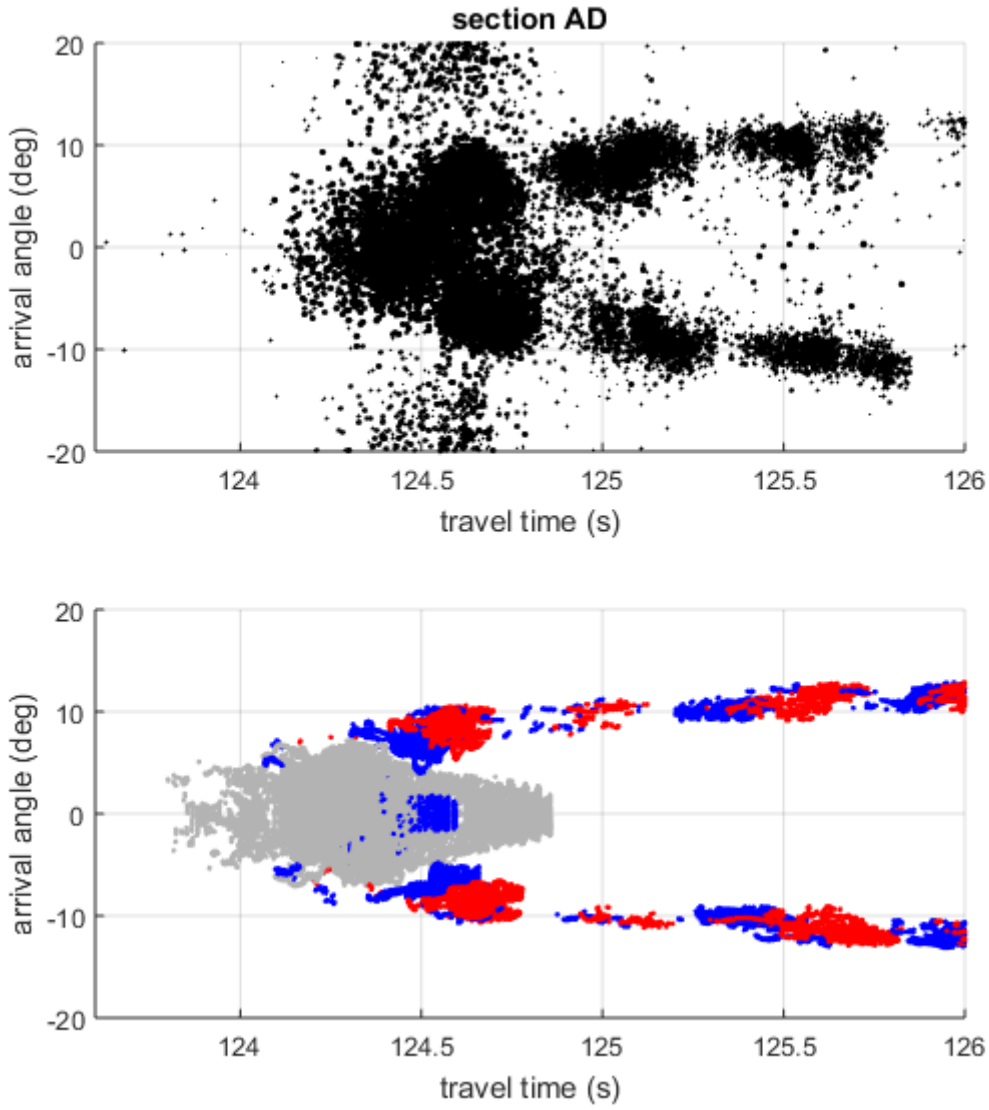

Figure 16: Observed acoustic arrival pattern for ACOBAR section AD as a function of travel time and arrival angle (upper panel). Predicted arrival pattern as a function of travel time and arrival angle for section AD from regional Fram Strait (lower panel), color coded by source angle. Red: source angle > 5°; gray: -5° < source angle < 5°; blue source angle > -5°

Figures 15 and 16 compare the observed acoustic arrival patterns for ACOBAR section AD with the predicted arrival patterns based on the Fram Strait regional ocean model. Observations show the sound channel arrivals first at low arrival angles followed by groups of 4 + 6 + 6 bottom-reflected arrivals. The predicted arrivals show the same basic pattern with the second set of bottom-reflected arrivals being more unstable than observed. The observations show a seasonal signal in the early arrivals. This seems to be also present in the model predictions, if slightly masked by the model drift. During cooling observed around yearday 830 early arrivals were observed to coincide with the first set of bottom-reflected arrivals. The model shows a similar event at yearday 730 and an even stronger event at yearday 470, where the early arrivals are actually crossing the first set of bottom-reflected arrivals. No arrival angle information is available for the observations during the first year of the experiment. It is therefore not possible to see if a similar event occurred in the observations of this year. Generally, the travel time of the early arrivals is more variable in the

model data as illustrated by Figure 16. This is partly due to the slight model drift. Both model and observations show additional early sound channel arrivals in the case of warming events, for example at yearday 300 in the model or on several occasions between yearday 670 and 770 in the observations. Short turn warming events in the observation and model are generally not coinciding in time. The model shows less short-turn variability than the observations, as is expected from the comparison of range-depth averaged temperatures (Figure 7).

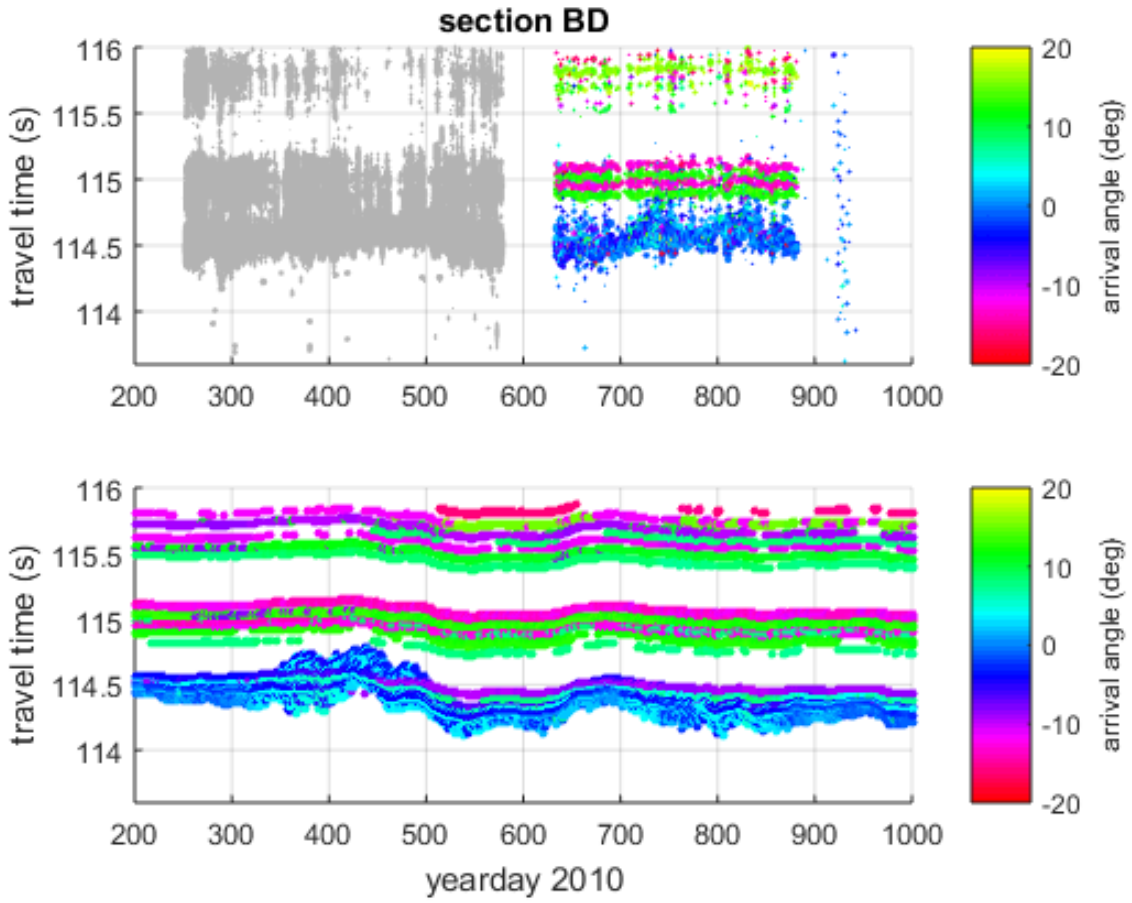

Figure 17: Observed time series of acoustic arrivals for ACOBAR section BD (upper panel) and predicted time series of arrivals for section BD from regional Fram Strait (lower panel). For the first deployment year of section BD no arrival angle information is available for the observations.

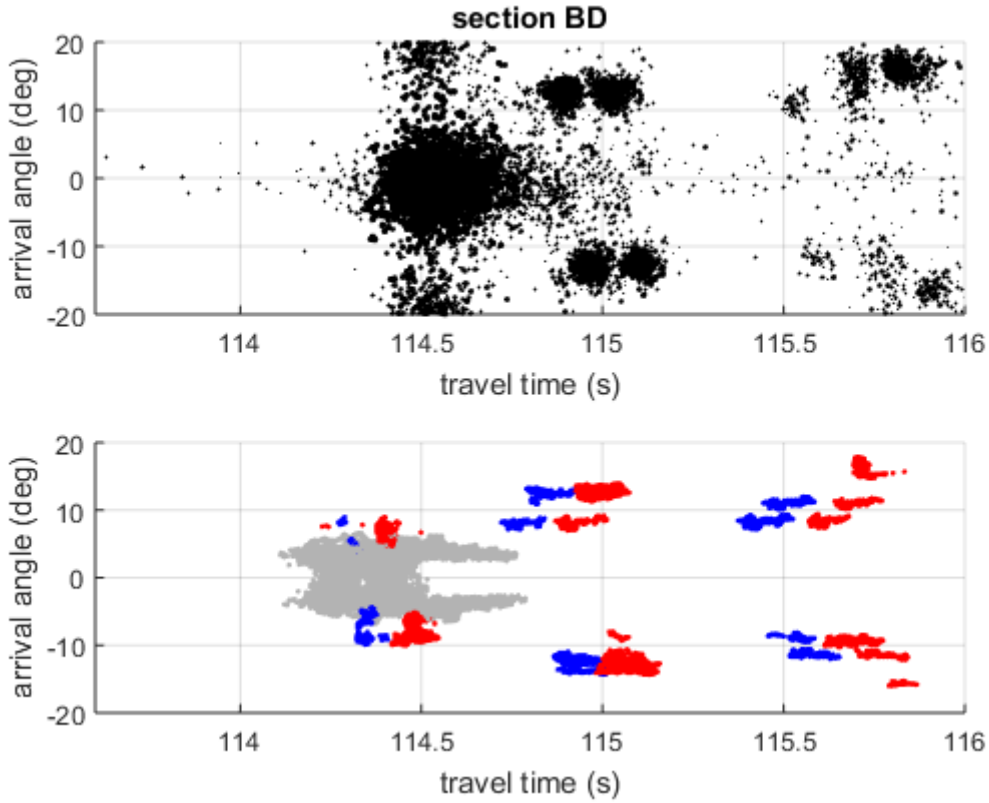

Figure 18: Observed acoustic arrival pattern for ACOBAR section BD as a function of travel time and arrival angle (upper panel). Predicted arrival pattern as a function of travel time and arrival angle for section BD from regional Fram Strait (lower panel), color coded by source angle. Red: source angle > 5°; gray: -5° < source angle < 5°; blue source angle > -5°

The arrivals for ACOBAR section BD are characterized by high temporal stability, especially the sets of bottom reflected arrivals are very stable in time. The patterns of observed and predicted arrivals match (Figure 15 and 16). The bottom-reflected arrivals between 115.5 and 116 s travel time are more intermittent in the observations than in the model predictions. The model predictions show that the yearly sound-channel arrivals are actually coinciding with a first set of deep-going arrivals. These are too close in arrival time and angle to the sound channel arrivals to be detected separately in the observations. Model arrivals are slightly earlier than observed arrivals. As for section AD the short-term variability of the sound channel arrivals is higher in the observations than in the model predictions. This agrees with the comparison of depth-range averaged temperatures in section 2.

For ACOBAR section BA there are more differences between the observed acoustic arrivals and the predicted arrival pattern based on the regional Fram Strait model. However, a close look reveals that these differences are mostly caused by predicted high-angle arrivals that are not registered in the observations. As these steep arrivals correspond to ray paths with multiple bottom reflections it can be assumed that the acoustic energy from these ray paths is dampened out. Other than the missing arrivals the predicted arrival structure is again very similar to the observations. The high-angle arrivals observed at 207.2-208 s travel time correspond in arrival time and angle to the predicted bottom-reflected arrivals from the regional Fram Strait model. Both model and observations show the early sound channel arrivals to be more widely spread for section BA than for the shorter sections AD and BD. This spread is assumed to be caused by scattering by small-scale oceanographic variability

(Dushaw et al., 2016). The regional Fram Strait model predicts bottom-reflected rays with positive arrival angles of about 10 degrees that are overlapping in travel time with the sound channel arrivals. These bottom-reflected arrivals can be observed during seasonal cooling events (yearday 400-550 and 800-850), when they are arriving earlier than the sound channel rays. They were not separable at the time of deployment in summer, when hydrographic section could be taken. **Thus, the ocean model makes it possible to identify and explain arrival pattern that could not be explained otherwise**. The comparison of arrival angle / travel time figures (Figure 18) makes it possible to also identify patterns that are hard to detect in the dot plots. For example, occasional arrivals form at 206.4 s travel time and -8 degree arrival angle can be identified as the intermittent arrival pattern predicted at 206.25-206.5 s travel time and -9 degrees arrival angle. The arrival pattern predicted at 206.4 – 207 s and at angles of +10 and -10 degrees is overlapping with the sound channel arrivals and not separable from these in the dot plots. In the arrival angle / travel time plot however, they can be identified because of the tilt between the positive and negative angle arrivals, with the positive angle arrivals arriving about 100 ms earlier that the negative angle arrivals. **This is very important information for inversion, as it proves that the assumption that all early arrivals belong to sound channel rays does not hold**.

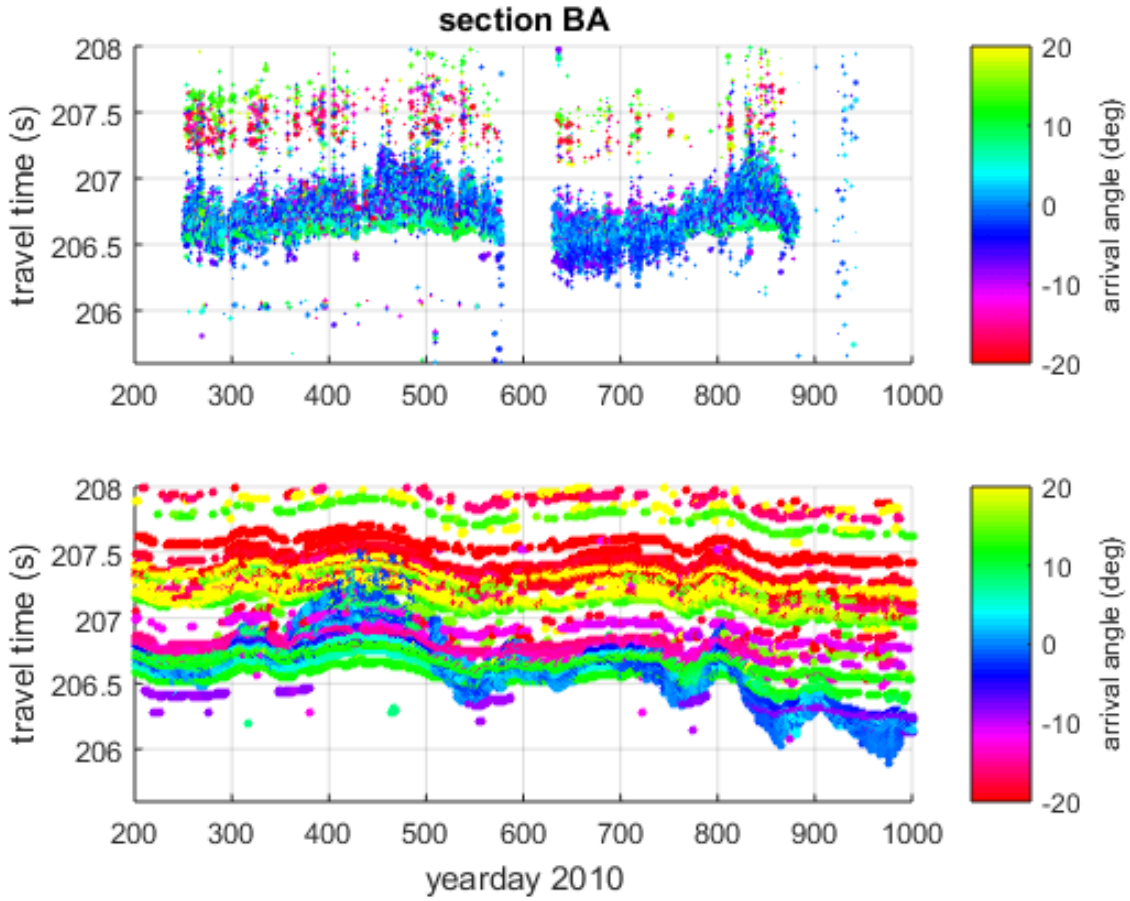

Figure 19: Observed time series of acoustic arrivals for ACOBAR section BA (upper panel) and predicted time series of arrivals for section BA from regional Fram Strait (lower panel)

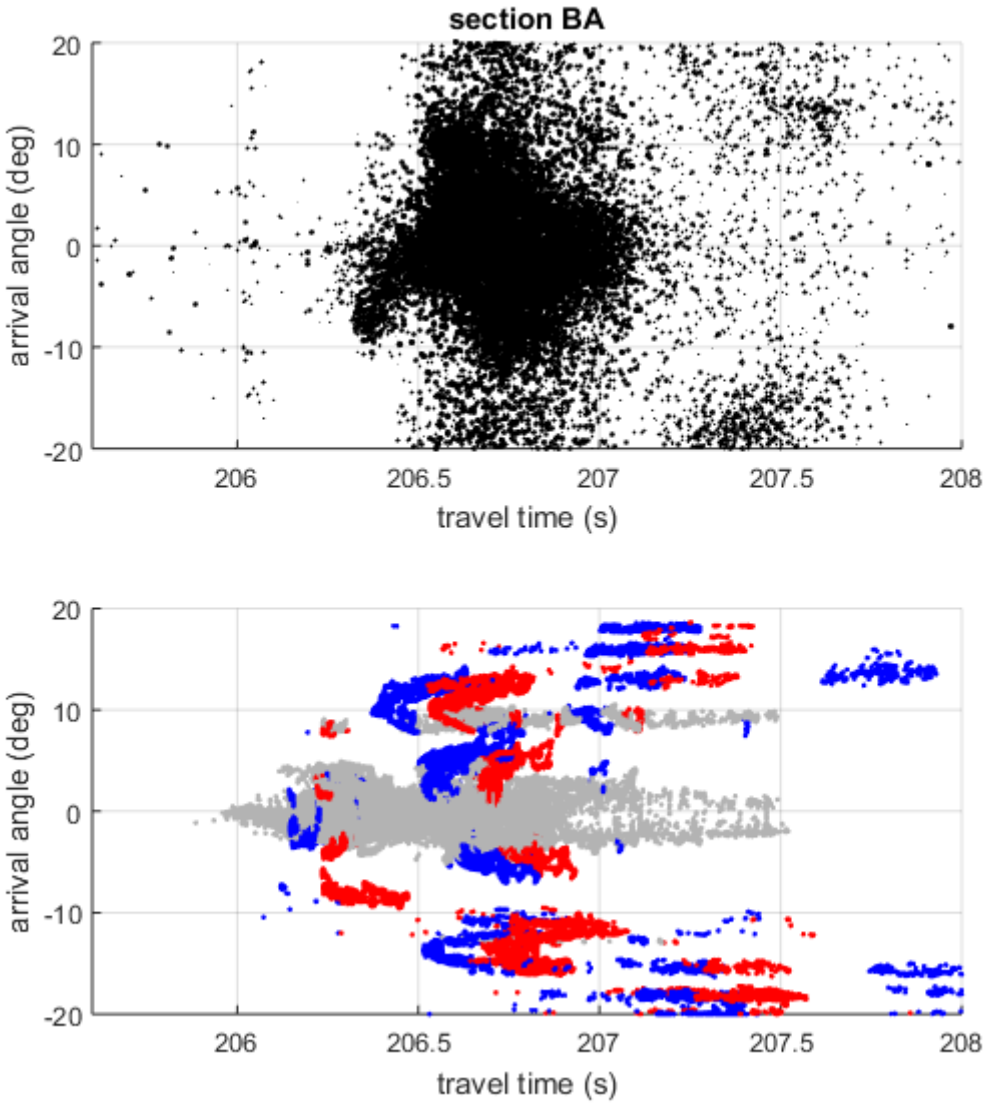

Figure 20: Observed acoustic arrival pattern for ACOBAR section BA as a function of travel time and arrival angle (upper panel). Predicted arrival pattern as a function of travel time and arrival angle for section BA from regional Fram Strait (lower panel), color coded by source angle. Red: source angle > 5°; gray: -5° < source angle < 5°; blue source angle > -5°

4.4 Conclusions for the assimilation of acoustic tomography data in Fram Strait

A high-resolution ocean model was Fram Strait was set up and evaluated. The model realistically describes ocean circulation and stratification in Fram Strait. Deviations to observations are explainable by limited model resolution preventing the eddy dynamics and its corresponding large-scale effects to be fully represented (Wekerle et al., 2017). The slight model drift seems not problematic at the time scales studied here. The ocean model can be used to correctly predict the observed acoustic arrival patterns. This makes the regional Fram Strait model an excellent tool to study the acoustic arrival pattern in Fram Strait and its temporal variability as well as the stability of the corresponding ray paths. This means that assumptions underlying both the assimilation and the inversion of acoustic tomography data can be tested.

The assessment of ray stability presented in this chapter highlighted the complexity of acoustic propagation in Fram Strait. The instability of the observed ray paths made it not recommendable to try to assimilate acoustic arrivals under the assumption of time-independent ray paths. While a statistic approach as used by Sagen and Dushaw for temperature inversions seems applicable, such an approach is not developed yet for data assimilation. In addition, the analysis of the acoustic arrival structure has shown that overlapping bottom-reflected and sound channel rays make the assumption of a purely statistical set of rays with essentially equal vertical ocean coverage somewhat simplified.

Because of the results of the analysis presented here, we decided to used inversion results (Sagen and Dushaw, 2017) instead of acoustic travel times for data assimilation. This also has the benefit of separating the technical issues of data assimilation and the choice of the modelled observational matrix. Data assimilation will first be tried using daily depth-range averaged sound speed derived from inverting the acoustic travel times of the three ACOBAR acoustic thermometry sections (A-B, A-D, B-D). The aim is to provide improved ocean heat flux estimates for the bidirectional water exchanges between the Nordic Seas and the Arctic Ocean through Fram Strait. The first step towards this is the comparison of depth-range averaged model temperatures to the inversion results and the comparison of Fram Strait heat fluxes to earlier model and observation-based estimates.

Efforts at setting up and testing the adjoint based 4-DVAR system for the Fram Strait model for assimilating depth-range averaged sound speeds along raypaths are ongoing at Scripps Institution of Oceanography. A first technical trial of the assimilation scheme has been successful. The analysis of the assimilation results will have to happen under a different project. Based on the success of the assimilation of depth-range averaged sound speeds for the ACOBAR acoustic tomography experiment, the methods developed here could be directly transferable to the UNDER-ICE acoustic tomography results. More advanced inversion schemes including bottom-reflected acoustic rays will be developed in the CANAPE-UNDER-ICE project. This would give additional depth-dependent information that can be used in future acoustic data assimilation efforts. It remains to be explored if more advanced assimilation techniques for the direct assimilation of acoustic travel times could be attempted in the future or if the conclusion here suggests that it is more convenient to separate the problems of assimilation and of establishing the corresponding observation matrix. Assimilation of inversion results certainly seems to be working and might open pathways to more routine implementation of use of acoustic tomography results by assimilating it into ocean state estimates such as ECCO.

For the trial assimilation experiment, we assimilated ray path AB for the period of 20 days from September 1 – 20, 2010. The model is initialized from ASTE state on September 1, 2010 and optimized the weighted data-model misfit (cost function) of depth averaged sound-speed in the 0-1000m along the ray paths. The cost function included only acoustic data and the tomography cost decreased by 87% over 10 iterative optimizations, adjusting the model depth-averaged sound speeds closer to the observations. A detailed analysis of the results and additional model-data comparisons assessing the impact of acoustic observations on ocean analysis and prediction will be performed under a different project

Ray ID	Model Cs for Iteration: 0	Model Cs for Iteration: 10	Data Cs	Weight
10	1462.432823776878	1460.545803980036	1460.720000000000	8.779100000000000
12	1462.532521177167	1460.225733129618	1460.855800000000	8.779100000000000
14	1462.678551829525	1460.025372763383	1460.717700000000	8.779100000000000
15	1462.748523831245	1459.966013155653	1458.124100000000	8.779100000000000
16	1462.785479614642	1459.920728977571	1460.597000000000	8.779100000000000
17	1462.814158178436	1459.943687887434	1458.124100000000	8.779100000000000
18	1462.847158683894	1460.053406174706	1460.689300000000	8.779100000000000
20	1462.879406094243	1460.358611565154	1460.859000000000	8.779100000000000
	Tomo cost: 583.8	Tomo cost: 76.57		

Table 3: test results for 20-day acoustic data assimilation of for 2010-09-01 to 20

5. References

Beszczynska-Möller, A., Fahrbach, E., Schauer, U., and Hansen, E. (**2012**). Variability in Atlantic water temperature and transport at the entrance to the Arctic Ocean, 1997–2010, *ICES Journal of Marine Science*, **69**, 852–863.

Bentsen, M., Bethke, I., Debernard, J. B., Iversen, T., Kirkevåg, A., Seland, Ø. Drange, H., Roelandt, C., Seierstad, I. A., Hoose, C., and Kristjansson, J. E. (**2013**). The Norwegian Earth System Model, NorESM1-M - Part 1: Description and basic evaluation of the physical climate, *Geosci. Model Dev.*, **6**, 687-720, doi:10.5194/gmd-6-687-2013

de Steur, L., Hansen, E., Gerdes, R., Karcher, M., Fahrbach, E., and Holfort, J. (**2009**). Freshwater fluxes in the East Greenland Current: A decade of observations, *Geophys. Res. Lett.*, **36**, L23611, doi:10.1029/2009GL041278

Dushaw, B. D. and Sagen, H. (**2016**). A comparative study of moored/point and acoustic tomography/integral observations of sound speed in Fram Strait using objective mapping techniques, *J. Atmos. Oceanic Tech.*, **33**, 2079-2093, doi:10.1175/JTECH-D-15-0251.1

Dushaw, B. D., Sagen, H., and Beszcsynska-Möller, A. (**2016**). On the effect of small-scale variability on the acoustic propagation in Fram Strait: The tomography forward problem, J. Acoust. Soc. Am., **140**, 1286-1299.

Dushaw, B. D. (**2017**). "Estimating temperature in Fram Strait using DAMOCLES and ACOBAR acoustic tomography data by exploiting small-scale variability," NERSC Technical Report 378, Nansen Environmental and Remote Sensing Center, Bergen, Norway, 6 November 2017, 43 pp.

Dushaw, B. D., and Sagen, H. (**2017**). The role of simulated small-scale ocean variability in inverse computations for ocean acoustic tomography, *J. Acoust. Soc. Am.*, **142**, 3541-3552, doi:10.1121/1.5016816.

Dzieciuch, M. A., Cornuelle, B. D., and Skarsoulis, E. K. (**2013**). Structure and stability of wave-theoretic kernels in the ocean, *J. Acoust. Soc. Am.*, **134**, 3318-3331.

Forget, G., Campin, J.-M., Heimbach, P., Hill, C. N., Ponte, R. M., and Wunsch, C. (**2015**a). ECCO version 4: an integrated framework for non-linear inverse modeling and global ocean state estimation, *Geoscientific Model Development*, **8**, 3653-3743.

Forget, G., Fukumori, I., Heimbach, P., Lee, T., Menemenlis, D., Ponte, R. M. (**2015**b). Estimating the Circulation and Climate of the Ocean (ECCO): Advancing CLIVAR Science, *CLIVAR Exchanges* No. 67, Vol. **19**, No. 2, 41-45.

Geyer, F., Yamakawa, A., Dzieciuch, M., and Sagen, H. (**2015**). Processing of acoustic tompgraphy data in the ACOBAR and UNDER-ICE experiments and development of new metadata structure for acoustic moorings, NERSC Technical report no **361**.

Hattermann, T., Isachsen, P. E., von Appen, W.-J., Albretsen, J., and Sundfjord, A. (**2016**). Eddy-driven recirculation of Atlantic Water in Fram Strait, *Geophys. Res. Lett.*, **43**, doi:10.1002/2016GL068323.

Langehaug, H. R., Geyer, F., Smedsrud, L. H.,and Gao, Y. (**2013**). Arctic sea ice decline and ice export in CMIP5 historical simulations, *Ocean Modelling*, **71**, 114-126.

Marnela, M., Rudels, B., Houssais, M.-N., Beszczynska-Möller, A., and Eriksson, P. B. (**2013**). Recirculation in the Fram Strait and transports of water in and north of the Fram Strait derived from CTD data, *Ocean Science*, **9**, 499-519.

Nguyen, A., Ocaña, V., Garg, V., Heimbach, P., Toole, J., Krishfield, R., et al. (**2017**). On the Benefit of Current and Future ALPS Data for Improving Arctic Coupled Ocean-Sea Ice State Estimation. Oceanography, **30**(2), 69–73, doi:10.5670/oceanog.2017.223

Sagen, H., Dushaw, B. D., Skarsoulis, E. K., Dumont, D., Dzieciuch, M. A., and Beszczynska-Möller, A. (**2016**): Time series of temperature in Fram Strait determined from the 2008–2009 DAMOCLES tomography measurements and an ocean model, *J. Geophys. Res. Oceans*, doi:10.1002/2015JC011591.

Sagen, H., Worcester, P. F., Dzieciuch, M. A., Geyer, F., Sandven, S., Babiker, M., Beszczynska-Möller, A., Dushaw, B. D., Cornuelle, B. (**2017**). Resolution, identification, and stability of breadband acoustic arrivals in Fram Strait, *J. Acoust. Soc. Am.*, **141** (3), 2055-2068, doi:10.1121/1.4978780.

Sakov, P., Counillon, F., Bertino, L., Lisæter, K. A., Oke, P. R., and Korablev, A. (**2012**). TOPAZ4: an ocean-sea ice data assimilation system for the North Atlantic and Arctic, *Ocean Science*, doi: 10.5194/os-8-633-2012

Skarsoulis, E., Piperakis, G., Kalogerakis, M., Sagen, H., Haugen, S. A., Beszczynska-Möller, A., and Worcester, P. F. (**2010**). Tomographic inversions from the Fram Strait 2008–9 experiment, in *Proceedings of the European Conference on Underwater Acoustics 2010* (Istanbul, Turkey), pp. 265–271.

Storheim, E., Sagen, H., Falck, E., Beszczynska-Möller, A. (**2018**). "UNDER-ICE data report", NERSC Technical report no **390**, rev. 1.0

von Appen, W.-J., Schauer, U., Hattermann, T., and Beszczynska-Möller, A. (**2016**). Seasonal cycle of mesoscale instability of the West Spitsbergen Current, *J. Phys. Oceanogr.*, doi:10.1175/JPO-D-15-0184.1.

Walczowski, W. (**2013**). Frontal structures in the West Spitsbergen Current margins, *Ocean Sci.*, **9**(6), 957–975.

Wekerle, C., Wang, Q., von Appen, W.-J., Danilov, S., Schourup-Kristensen, V., and Jung, T. (**2017**). Eddy-resolving simulation of the Atlantic Water circulation in the Fram Strait with focus on the seasonal cycle. *JGR Oceans*, **122**, 8385–8405. https://doi.org/10.1002/2017JC012974

Yamakawa, A., Sagen, H., Babiker, M., Worcester, P.F. and Furevik, B.R. (**2016**). Soundscape Characterization and the Impact of Environmental Factors in the Central Part of the Fram Strait. *Proceedings of the Institute of Acoustic*, Vol. **38**, Pt. 3, 187-194, Cambridge, UK.